

Spin dependent scattering of a domain-wall of controlled size.

J.-E. Wegrowe^{a)}, A. Comment, Y. Jaccard, J.-Ph. Ansermet

Institut de Physique Expérimentale, Ecole Polytechnique Fédérale de Lausanne, CH - 1015 Lausanne, Switzerland.

N. M. Dempsey, J.-P. Nozières

Laboratoire de magnétisme Louis Néel, CNRS, BP166X 38042 Grenoble, France.

(October 8, 2018)

Magnetoresistance measurements in the CPP geometry have been performed on single electrodeposited Co nanowires exchange biased on one side by a sputtered amorphous GdCo_{1.6} layer. This geometry allows the stabilization of a single domain wall in the Co wire, the thickness of which can be controlled by an external magnetic field. Comparing magnetization, resistivity, and magnetoresistance studies of single Co nanowires, of GdCo_{1.6} layers, and of the coupled system, gives evidence for an additional contribution to the magnetoresistance when the domain wall is compressed by a magnetic field. This contribution is interpreted as the spin dependent scattering within the domain wall when the wall thickness becomes smaller than the spin diffusion length.

I. INTRODUCTION

Spin dependent scattering studies emerged with the first realizations of magnetic nanostructures, and gave rise to the discovery on spin injection [1], Giant magnetoresistance (GMR) [2,3] and tunneling magnetoresistance (TMR) [4]. In ferromagnets, Spin polarization of the current is due to spin-flip scattering which favors the orientation of the conduction electron spins in the direction of the magnetization. When a change of magnetization occurs at the nanoscopic scale, the spins of conduction electrons relax from the initial to the final direction of the magnetization, and this relaxation leads to an supplementary resistance [1,5,6]. However, this relaxation takes place only in the case of an abrupt spatial change of the magnetization, namely a length smaller or equal to the spin diffusion length l_{sf} (about 20 nm in Co measured with Co/Cu/Co multilayers) [7,8]. In the case of a smooth magnetic change, the polarization axis of the conduction electrons follows the local magnetic field adiabatically [9,10] and there is no relaxation.

The spin relaxation in artificial magnetic multilayers with anti-parallel coupling has been studied extensively both at the experimental and theoretical level due to the large magnetoresistance observed (the so-called GMR) [11]. However, in the case of non uniformly magnetized layers, or domain-walls (the so-called Domain-wall Scattering problem: DWS), the relaxation has not been evidenced clearly. Different theoretical models were proposed and are currently under development [10,12–14]. Simply speaking, two regimes have to be considered depending on the domain-wall thickness δ . On one hand, for domain-wall thickness larger than a characteristic length (let say $\delta > l_{sf}$), the spin polarization axis rotates adiabatically and hence no supplementary resistance is

expected. On the other hand, as δ approaches this characteristic length, a progressive enhancement of the relaxation occurs, resulting in an additional magnetoresistance contribution.

Several attempts were recently made to measure the DWS [15–20]. The main difficulty of these studies appears to be due to the importance of the bulk anisotropic magnetoresistance (AMR) which is due to the anisotropy of the spin-orbit scattering, with respect to the direction of the current [21,22]. In order to correct the AMR contribution, the micromagnetic configurations have to be determined with great precision. However, the domain-walls are present at low field, where other non uniform spin configurations usually coexists (like flux closures). Furthermore, at low external field the domain-wall thickness is defined by the local magnetostatic and anisotropy field, and can not be controlled easily.

The aim of the present study is to measure the DWS in a nanoscopic domain-wall the thickness of which can be controlled by a strong external magnetic field. The measurement is performed in the Current Perpendicular to the domain-wall (CPW) geometry according to a procedure already developed for measuring single nanowires [23]. A "Zeeman Domain-wall" was constructed by employing a ferrimagnetic amorphous GdCo_{1.6} alloy as a pinning layer on one side of a Co nanowire. In amorphous GdCo alloys at low temperature, the magnetic moments of Gd (about $7 \mu_B$) and of Co (about $2 \mu_B$) are aligned ferrimagnetically. When the Gd contribution predominates (which is the case here), the Co moments are always aligned anti-parallel with respect to an external magnetic field, as long as the amplitude of the field is smaller than the Gd-Co atomic exchange field (see Fig.1(a)). Consequently, near the GdCo_{1.6}/Co interface, where the Co-Co exchange is dominant, a stable 180 domain-wall, which is compressed by the external field, exists in the Co sublat-

tice. Details of the micromagnetic configuration of such bilayers can be found in [24,25].

The structure of this paper is the following. The samples preparation (Section I) is first described. The magnetization characterization (Section II), the temperature dependence of the resistivity (Part III), and the magnetoresistance (Section IV) of (A) Co nanowires, (B) $\text{GdCo}_{1.6}$ thin films, and (C) hybrid Co/ $\text{GdCo}_{1.6}$ samples are then reported. Analyse and discussion about the action of the interface and domain-wall scattering follow in Section V. The domain-wall thickness $\delta(H, T)$ is evaluated by using a simple model. A scaling plot $R(\delta(H, T))$ yields the MR as a function of the domain-wall thickness.

II. SAMPLES PREPARATION

Nanocrystallized Co nanowires are obtained by electrodeposition in track etched membrane templates [26]. Polyester membranes with about $6 \cdot 10^8$ pores/ cm^2 were used. The wires are about 6000 nm in length and 80 nm in diameter. An in-situ technique, inside the electrolytic bath, allows a sub-micron contact to be made, in order to measure one single nanowire [23]. The detailed procedure is as follows:

(1) One surface (called in the following S2) of the membrane is recovered by a 200 nm thick sputtered gold layer. This surface plays the role of working electrode during the Co electrodeposition. The other surface (surface S1 in Fig.1(b)) is open to the Co electrolytic bath. The pores are filled with Co up to about a third of the pores length.

(2) After cleaning the surface S2 with potassium cyanide (KCN) in order to dissolve totally the gold electrode, a film of 220 nm amorphous GdCo is sputtered at room temperature from a GdCo_2 target. The GdCo layer is hence in contact with the bottom of the Co wires. A 20 nm Mo protection layer is deposited on the GdCo film to avoid oxidation.

(3) A gold film of 50 nm is sputtered on the surface S1 in order to control the potential between the two surfaces of the membrane during electrodeposition. This thin layer does not obstruct the pores. The surface S2 play the role of working electrode again. The surface S1 and the top of the Co wires are cleaned by "ex-situ" reduction in a NaCl electrolytic bath in order to remove the skin of the Co oxide. (4) The rest of the pores are filled with Co while controlling the voltage between the surfaces S1 and S2. A single contact is obtained by a feed-back loop which stops the deposition as soon as the voltage reaches zero (i.e. when the first wire connects to the surface S1).

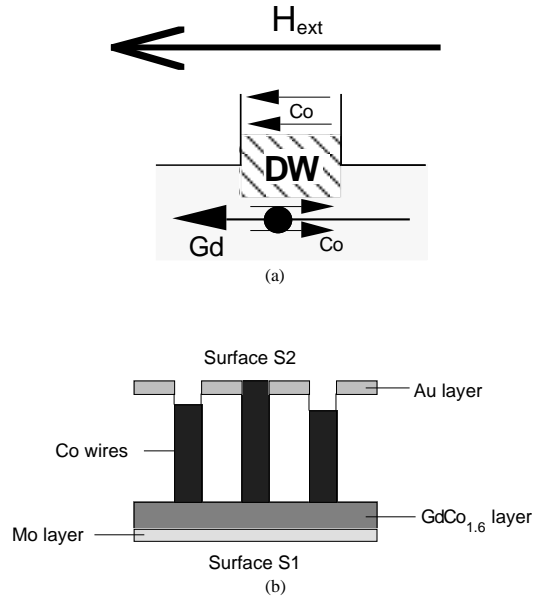


fig1.eps

FIG. 1. (a) Schematic diagram of an interface between a Co wire and the $\text{GdCo}_{1.6}$ layer. The presence of a 180° domain wall is evidenced by the hatched zone. (b) General structure of the hybrid GdCo/Co system.

The ferromagnetic wires obtained by this method have been characterized by various techniques, including NMR spectroscopy and X ray diffraction [27]. It was shown that the Co is nano-crystallized with a broad size distribution of crystallites sizes and with a mixture of fcc and hcp phases. The GdCo_x layer stoichiometry was estimated, by electron dispersive x-ray (EDX) analysis, to be $\text{GdCo}_{1.6}$.

III. MAGNETIC CHARACTERIZATION

A. Co nanowires

The magnetic characterization of the Co wires has been performed on a membrane (containing about 10^7 nanowires), with the field perpendicular to the wires axes (Fig.2). It has been shown that the magnetocrystalline anisotropy direction of the crystallites are distributed perpendicular to the wire axis, due to strains and magnetostriction during the growth within the pores [28]. The remanent state is not uniformly magnetized along the wire axis, and a domain-wall or vortex is present [29]. The spin configuration of this state is very sensitive to the nanocrystalline configuration.

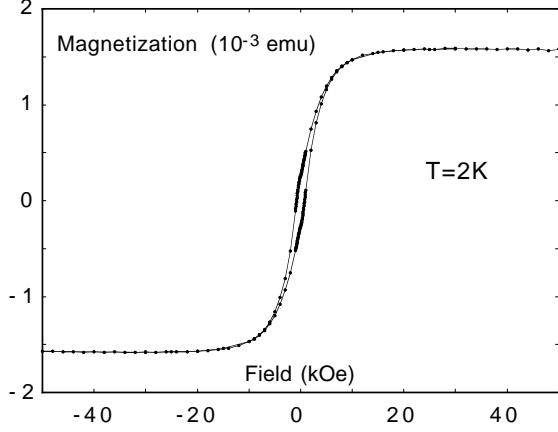


FIG. 2. Hysteresis loop of a membrane with about 10^7 Co nanowires, measured at 2 K , with the applied field perpendicular to the wire.

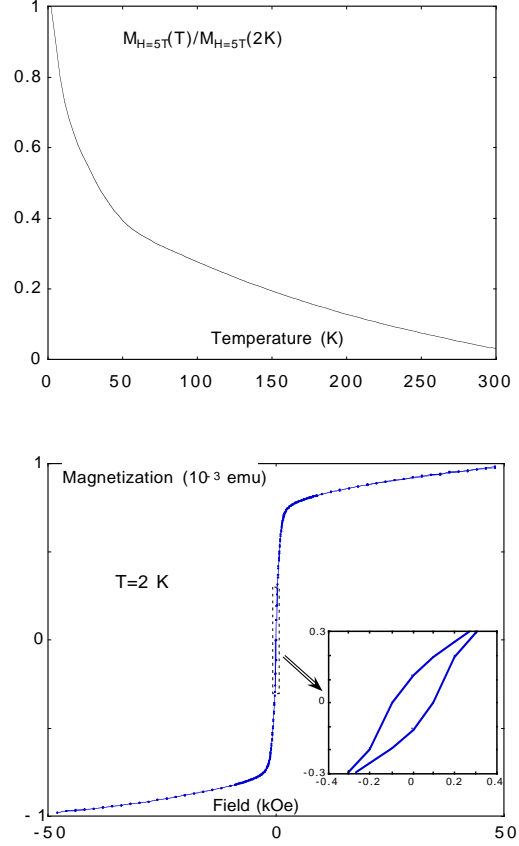


FIG. 3. (a) Temperature dependence of the magnetization of a $\text{GdCo}_{1.6}$ layer measured at $H = 5\text{ T}$ in the plane of the layer. (b) hysteresis loop of the $\text{GdCo}_{1.6}$ layer measured at 2 K in the plane of the layer.

B. $\text{GdCo}_{1.6}$ thin films

The temperature dependence of the $\text{GdCo}_{1.6}$ has been reported in reference [30]. The magnetic moment is almost zero at room temperature and increases with decreasing temperature, according to the curve of Fig.3(a), measured under a 5 T external field. The shape of the magnetic hysteresis loop at 2 K show that the magnetization at 5 T is not the saturation magnetization, as expected for ferrimagnetic materials (Fig.3(b)).

C. $\text{GdCo}_{1.6}/\text{Co}$ hybrid structures

At high temperature, $\text{GdCo}_{1.6}$ moment is too weak to provide a measurable exchange bias. The hybrid structure therefore behaves like the Co nanowires. The magnetic hysteresis loop of the hybrid structure at 2 K is shown in fig.4, with to the sum of the individual contribution of the Co nanowires and the $\text{GdCo}_{1.6}$ layer. The difference between the two curves of fig.4 (hatched area in Fig4) is due to the effect of the exchange biasing at the interface, leading to the creation of a large domain-wall at low field. The magnetic curve of the hybrid structure can hence be described, in a first approximation, by the relation

$$M_{\text{GdCo}_{1.6}/\text{Co}}(H) = M_{\text{GdCo}_{1.6}}(H) + [1 - \delta(H)/L] \cdot M_{\text{Co}}(H) \quad (1)$$

where L is the total length of the Co wire i.e. $L = 6000\text{ nm}$. Above 3 T , the two loops are superimposed.

The contribution of the domain-wall $\delta(H)/L$ is hence negligible for $H > 3T$: the contribution of the DW to the AMR should hence be also negligible at high field.

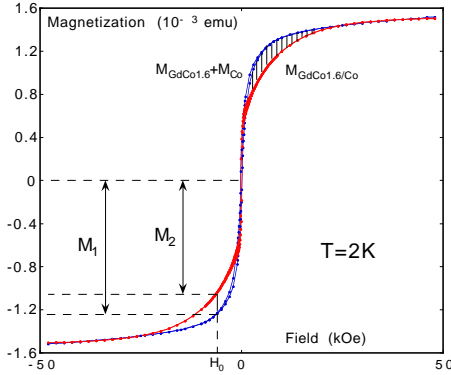


FIG. 4. 2 K hysteresis loop of the $\text{GdCo}_{1.6}/\text{Co}$ hybrid structure superimposed with the sum of the individual hysteresis loops of the Co wire and the $\text{GdCo}_{1.6}$ layer. The difference $M_1 - M_2$ (hatched area) is the contribution of the low field domain wall.

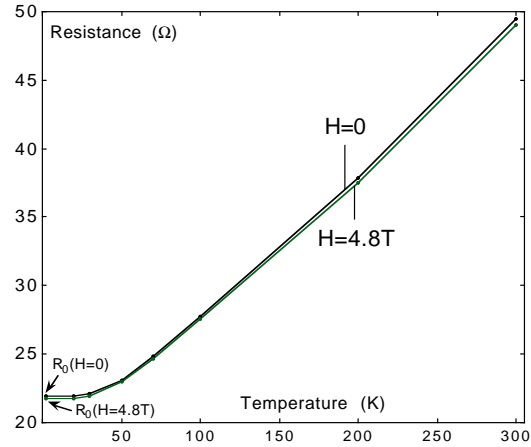


FIG. 5. Temperature dependence of the resistance of the Co nanowire at $H = 0$ and $H = 4.8T$.

B. $\text{GdCo}_{1.6}$ thin films

IV. ELECTRICAL CHARACTERIZATION

A. Co nanowires

Resistivity measurements have been performed on Co samples. The general temperature profile is plotted in Fig.5. The value of the resistance, (50 Ω), indicates that two or three wires are contacted in parallel in this sample. The general profile is in accordance with the behavior expected for bulk Co. The contribution due to phonon scattering is linear and the curvature is due to the spin-disorder resistivity, observable only at high temperature [31]. The residual resistivity R_0 is rather sensitive to the Co nanocrystalline structure and the quality of the micro-contact, which are seldom reproducible from one wire to another.

The transport properties are measured in the current-in-plan geometry (CIP) with the standard 4 probe technique. The resistance of the thin films in this configuration is of the order of 5 Ω at room temperature. The low temperature profile (Fig. 6), well reproducible, shows a typical feature, characteristic of the "structural Kondo effect" [32,33]: this profile does not depend on the external magnetic field (see section IV), and hence it is not caused by spin dependent scattering. In contrast to the magnetic Kondo effect, where the negative thermal coefficient of the resistivity is due to magnetic impurities dilute in non-magnetic metals, the "structural Kondo effect" is due (in an oversimplified picture [33]) to another degree of freedom present in disordered systems. The temperature dependence of the resistivity below about 20 K follows the form $\rho(T) = -\alpha \cdot \ln(k_B^2 T^2 + \Delta^2) + \beta$ where α is a positive coefficient, k_B the Boltzmann constant and Δ, β constants. This behaviour is in agreement with previous studies on Gd-Co amorphous films [34].

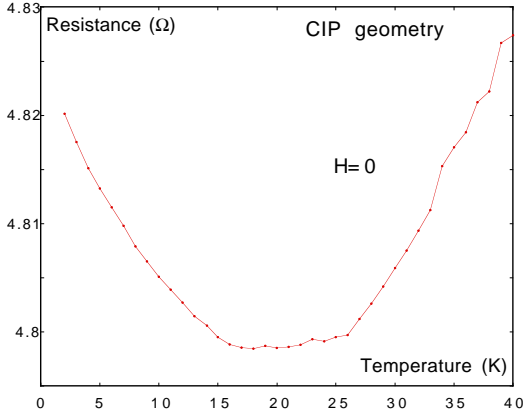


FIG. 6. Temperature dependence of the resistance of a $\text{GdCo}_{1.6}$ layer at $H = 0$, measured in CIP geometry.

C. $\text{GdCo}_{1.6}/\text{Co}$ hybrid structures

The resistance of the hybrid structure is about 180Ω at room temperature. The contributions of the Co wire and of the $\text{GdCo}_{1.6}$ film are observed in the temperature dependence of the resistance (Fig.7). From 300 K down to 50 K , the profile follows the usual bulk Co curve, while below $T_{\min} = 20 \text{ K}$ the structural Kondo effect dominates (inset of Fig.7) at zero magnetic field and 4.8 T magnetic field.

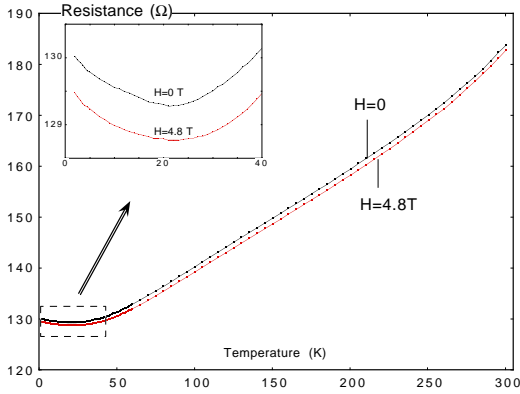


FIG. 7. Temperature dependence of the resistance of the hybrid structure at $H = 0$ and $H = 4.8 \text{ T}$. Inset: low temperature zoom.

V. MAGNETORESISTANCE

A. Co nanowires

The magnetoresistive hysteresis loops of isolated Co wires at different temperatures are shown in Fig.8. The magnetoresistance is normalized with respect to the zero

field resistance $R(H = 0)$ at each temperature. The room temperature magnetoresistance has been studied in detail elsewhere [28]. The behavior observed is typical of anisotropic magnetoresistance (AMR) in which the resistance increases as the magnetization is aligned with the current. If ϕ is the angle between the current and the magnetization $M(H)$, the magnetoresistance hysteresis loop is linked to the magnetic hysteresis loop in the wire by the relation $\Delta R(H) = R_0 + \Delta R_{\max} \cos^2(\phi(H))$. The jumps of the magnetization show the unstable states corresponding to the nucleation and the annihilation of domain-walls (Fig.8).

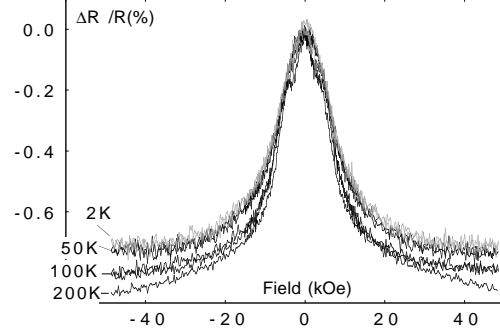


FIG. 8. Magnetoresistance of a Co wire, normalized at $R(H = 0) = 50 \Omega$.

On the other hand, the high field magnetoresistance shows an important temperature dependence. As shown in Fig.9, the quantity $\Delta^{4.8}R = R(H = 0) - R(H = 4.8 \text{ T})$ decreases linearly from 300 K ($\Delta^{4.8}R \approx 0.4 \Omega$) down to about 50 K ($\Delta^{4.8}R \approx 0.17 \Omega$). This MR contribution is opposite to the Lorentz magnetoresistance. It is characterized by the fact that the increase of the field reduces the resistivity in the same way that the decrease of the temperature does. This behaviour may be explained by the spin-disorder, which contribution can be seen in the temperature dependence of the resistivity (Fig.5). The magnetoresistance due to this contribution is poorly understood. However, below 60 K , the effect disappears and $\Delta^{4.8}R(T)$ is roughly constant. In the following, we will focus on the low temperature region only: $T < 60 \text{ K}$.

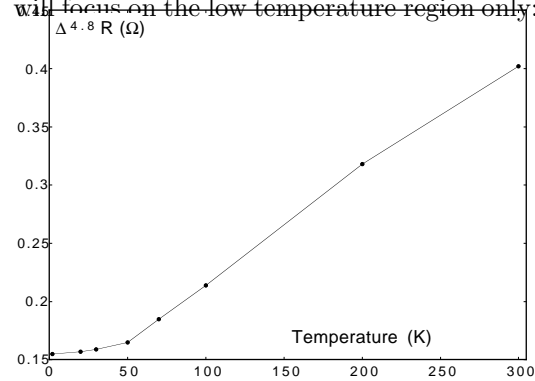


FIG. 9. Temperature dependence of the anisotropic Co magnetoresistance $\Delta^{4.8}R = R(H = 0) - R(H = 4.8 \text{ T})$.

B. GdCo_{1.6} thin films

The low temperature magnetoresistance of GdCo thin films is reported in figure 10a and 10b for $H \perp I$ and $H // I$, respectively. Note that the asymmetry observed in Fig.10(a) is not relevant, as it is due to Hall currents in the 4 probe geometry. The magnitude of $\Delta^{4.8}R$ is quite similar and very small in the both configurations. The two magnetoresistance curves at 60K and 2K are approximately superimposed, and only a weak AMR contribution can be observed (Fig.10(a)). This is in accordance with the interpretation of section III(B) in terms of "structural Kondo effect": there is no thermal dependence of this magnetoresistance.

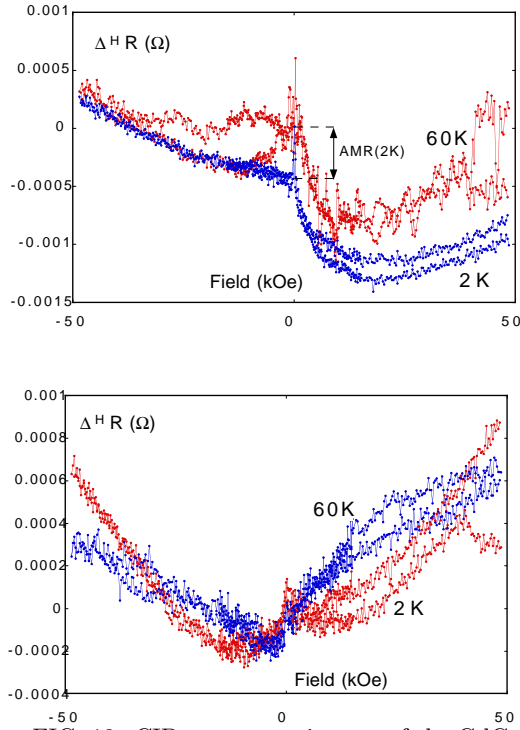


FIG. 10. CIP magnetoresistance of the GdCo_{1.6} layer with (a) the applied field perpendicular to the current and (b) the applied field parallel to the current.

C. GdCo_{1.6}/Co hybrid structures

The magnetoresistance hysteresis loop is shown in Fig.11. Due to the exchange biasing, the switching fields are lowered (Fig.11(b)) with respect to the Co switching fields, and a temperature variations of the remanent states can be observed. These effects are due to the temperature dependence of the exchange biasing at low field. The resulting magnetic configurations at the interface are very difficult to describe, and the contribution of the

DWS, if any, cannot be extracted from the AMR at low field.

On the other hand, at high field ($H > 3T$), it has been shown that the contribution of the DW to the magnetization (Section II(C)), and hence to the AMR, is negligible. Since the (CIP) magnetoresistance of the GdCo_{1.6} thin film is of the order of 10^{-3} % of the total resistance (Section above), the magnetoresistance of the hybrid structures is expected to be identical to that of isolated Co wires at high field.

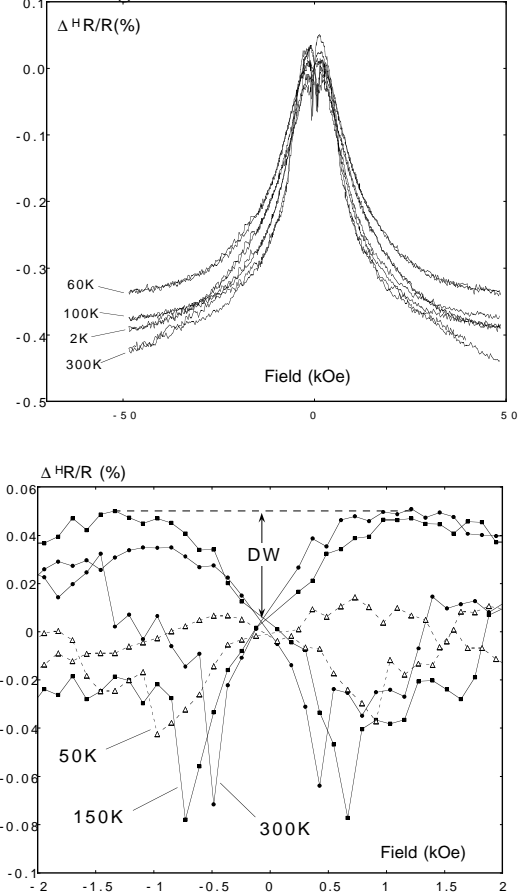


FIG. 11. (a) Magnetoresistance of the GdCo_{1.6}/Co hybrid structure, normalized at $R(H = 0) = 180 \Omega$. (b) low field zoom.

However, the high field magnetoresistance $\Delta^H R/R$ behavior is not as expected (Fig.11(a)). If the decrease of the AMR ratio, from 300 K down to 60 K is in accordance with the observation on the Co samples, the minimum of the high field magnetoresistance at about $T = 60 K$ is surprising. This temperature dependence is replotted in terms of magnetoresistance $\Delta^H R(T)$ (Fig.12) for different applied fields.

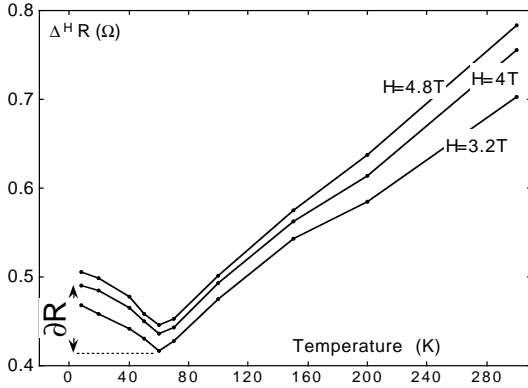


FIG. 12. Temperature dependence of the GdCo_{1.6}/Co hybrid structure magnetoresistance $\Delta^H R = R(H=0) - R(H)$ at various fields H .

Clearly, the negative temperature coefficient of the magnetoresistance below 60K must be related to the GdCo/Co interface. Note that this "positive" magnetoresistance (the resistance increases with the field) corresponds to the so-called "negative" magnetoresistance of the literature about DWS, because in contrast to our system, domain-walls usually disappear on increasing the external field.

VI. ANALYSIS AND DISCUSSION

Is it possible to interpret the negative slope of the magnetoresistance $\Delta^H R(T)$ (Fig.12) at low temperature and high field as the increasing contribution of the DWS produced by the compression of the domain-wall? As the MR of the amorphous GdCo_{1.6} layer is rather exotic and poorly understood, the effect may also be the manifestation of the structural disorder produced by the interface, and not by the domain-wall itself.

Let us first define the supplementary contribution to the magnetoresistance $\partial R(H, T)$. The reference point is taken with respect to the minimum of the $\Delta^H R(T)$ curve at 60 K and 3.2 T (see Fig. 12) :

$$\partial R(H, T) = \Delta^H R(T) - \Delta^{3.2} R(60 K) \quad (2)$$

Note that the reference point is chosen with respect to the minimum of the $\Delta^H R(T)$ curve at 60 K and 3.2 T which are expected to be the temperature and the field limits for the DW contribution (see paragraphs II(C) and IV). Equation (2) describes the MR of the GdCo/Co interface if we assume that the Co magnetoresistance $\Delta^H R(T)$ is constant below 60K (see Fig. 9). The magnetoresistance is then expressed in terms of the domain-wall size $\delta(H, T)$, with the following relation [35] :

$$\delta(H, T) = \pi \sqrt{\frac{(M_s^{Co} + M_s^{GdCo1.6}(T))A}{2 M_s^{Co} \cdot M_s^{GdCo1.6}(T) \cdot H}} \quad (3)$$

where M_s^{Co} is the saturation magnetization of Co (assumed constant in this temperature range), $M_s^{GdCo1.6}(T)$ the temperature dependent saturation magnetization of GdCo_{1.6} deduced from the Fig.3, A the exchange constant of Co, and H the applied magnetic field. This relation was obtained by minimizing the Zeeman and domain wall energies. The anisotropy contribution is neglected (approximation valid at $H > 3 T$), and the domain-wall is assumed to be centered at the interface. The magnetization $M_s^{GdCo1.6}(T)$ is given by the curve of Fig.3. From the values of the alloy density ($\rho = 7 g/cm^3$ [29]) and the alloy momentum ($\mu_{GdCo1.6}(2 K) = 5 \mu_B$ [29]), we obtain $M_s^{GdCo1.6}(2 K) = 775 emu/cm^3$.

The scaling plot $\partial R(\delta(H, T))$ is presented in Fig.13 without any adjustable parameter (we took $A = 0.85 \cdot 10^{-6} erg/cm$ [36] and $M_s^{Co} = 1430 emu/cm^3$ [37]). The scaling is rather good as the data are approximately aligned, which corroborates the validity of the hypothesis. The scaling plot corresponds to a domain wall size ranging from $\delta = 10 nm$ down to $\delta = 5 nm$, which is the range of the spin diffusion length l_{sf} of Co measured in multilayered Cu/Co nanowires [7]. The resistance of a 5 nm thick domain-wall is about $\partial R(4.8 T, 2 K) = 0.1 \Omega$.

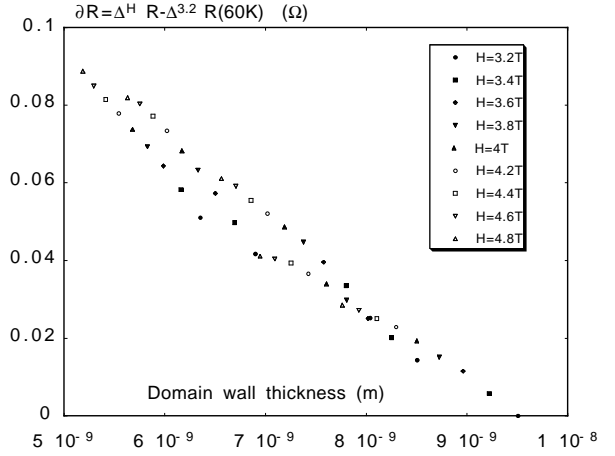


FIG. 13. Scaling plot of the enhanced magnetoresistance $\partial R(H, T) = \Delta^H R(T) - \Delta^{3.2} R(60 K)$, as a function of the domain wall thickness δ .

This result is in agreement with the estimation of the maximum interface resistance expected (i.e. in the case of infinitely thin domain wall) [5,6] :

$$R^{GMR} = 2 \rho \beta^2 l_{sf} / S \quad (4)$$

where β is the conductivity asymmetry, l_{sf} is the spin diffusion length and S is the section of the wire ($S = 5 \cdot 10^{-15} cm^2$). With taking the values measured previously on multilayered nanowires obtained with the

same electrodeposition method $\rho = 10^{-7} m\Omega$, $\beta = 0.45$, $l_{sf} = 20 nm$ [7,8] we have $R^{GMR} = 0.2 \Omega$.

Unfortunately, the small δ range in Fig13 and the rough scaling procedure do not allow to differentiate between the predictions $\partial R(\delta) \propto \delta^{-2}$ (Levy and Zang in reference [10]) or $\partial R(\delta) \propto \delta^{-1}$ and $\partial R(\delta) \propto -\delta$ (van Hoof et al. in reference [12]).

VII. CONCLUSION

Magnetic and transport properties have been measured on Co nanowires, on GdCo_{1.6} thin films and on exchange coupled systems GdCo_{1.6}/Co. The ferromagnetic Co-Co exchange coupling at a GdCo_{1.6}/Co interface induces the existence of domain-wall the thickness of which can be controlled with both the external magnetic field and the temperature. An additional contribution to the magnetoresistance due to the presence of this domain wall has been clearly evidenced. This domain wall magnetoresistance increases both with increasing the magnetic field strength, and with decreasing temperature (the latter below 60 K only).

A simple scaling procedure leads one to express the domain wall magnetoresistance as a function of the domain-wall thickness. The reasonable accuracy of the scaling shows that the magnetoresistance enhancement is indeed due to the compression of the DW by the external field and/or temperature.

The maximum domain wall contribution to the resistance of the GdCo_{1.6}/Co system is of the order of 0.1 Ω (0.5 % of the wire), in accordance with the GMR contribution of an ideal antiparallel ferromagnetic interface.

ACKNOWLEDGMENTS

We are grateful to H. Kind (IPE,EPFL) for helping to prepare potassium cyanide bath. We thank U. Rüdiger and G. E. W. Bauer for helpful discussions.

^{a)} e-mail:jean-eric.wegrowe@epfl.ch

- [1] M. Johnson and R. H. Silsbee, Phys. Rev. Lett. **55**, 1790 (1985) and M. Johnson and R.H. Silsbee Phys. Rev. B **37**, 4959 (1987).
- [2] M. N. Baibich, J. M. Broto, A. Fert, F. Nguyen Van Dau, F. Petroff, Phys. Rev. Lett. **61**, 2472 (1988).
- [3] G. Binash, P. Grünberg, F. Saurenbach, W. Zinn, Phys. Rev. B **39**, 4828 (1989).
- [4] J. S. Moodera, L.R. Kinder, T. M. Kinder T. M. Wing, R. Maserve, Phys. Rev. Lett. **74**, 3273 (1995).
- [5] P. C. van Son, H. van Kampen, P. Wyder, Phys. Rev. Lett. **58**, 7113 (1987).
- [6] T. Valet, A. Fert, Phys. Rev. B **48**, 7099 (1993).
- [7] L. Piraux, S. Dubois, C. Marchal, J.M. Beuken, L. Filipozzi, J.F. Despres, K. Ounadjela, A. Fert, J. Magn. Magn. Mat. **156**, 317 (1996).
- [8] B. Doudin, A. Blondel, J.-Ph. Ansermet, J. Appl. Phys. **79**, 6090 (1996) and B. Voegeli, A. Blondel, B. Doudin, J.-Ph. Ansermet, J. Magn. Magn. Mat. **151**, 388 (1995).
- [9] J. F. Gregg, W. Allen, K. Ounadjela, M. Viret, M. Hehn, S.M. Thompson, J. M. D. Coey, Phys. Rev. Lett. **77**, 1580 (1996).
- [10] P. Levy and Shufeng Zhang, Phys. Rev. Lett. **79**, 5111 (1997).
- [11] M. A. M. Gijs, G. E. W. Bauer, Adv. Phys. **46**, 285 (1997), J.-Ph. Ansermet, J. Phys. Cond. Mat. **10**, 6027 (1998) and references therein.
- [12] J. B. A. N. van Hoof, K. M. Schep, A. Brataas, P. J. Kelly, G. E. W. Bauer, Phys. Rev. B **59**, 138 (1999).
- [13] G. Tatara and H. Fukuyama, Phys. Rev. Lett. **78**, 3773 (1997).
- [14] A. Brataas, G. Tatara, G. E. W. Bauer, Phys. Rev. B **60**, 3406 (1999) and A. Brataas, G. Tatara, G. E. W. Bauer, Phys. Mag. B **78**, 545 (1998).
- [15] U. Rüdiger, J. Yu, L. Thomas, S. S. P. Parkin, A. D. Kent, Phys. Rev. B **59**, 11914(1999) and U. Rüdiger, J. Yu, A. D. Kent, S. S. P. Parkin, J. Appl. Phys. **73**, 1298 (1998).
- [16] T. Taniyama, I. Nakatani, T. Namikawa, Y. Yamazaki, Phys. Rev. Lett. **82**, 2780 (1999).
- [17] K. Mibu, T. Nagahama, T. Shinjo, T. Ono, Phys. Rev. B **58**, 6442 (1998).
- [18] Kimin Hong, N. Giordano, J. Phys. Cond. Mat. **10**, L401 (1998).
- [19] U. Rüdiger, J. Yu., S. Zhang, A. D. Kent, S. S. P. Parkin, Phys. Rev. Lett. **80** 1116 (1998).
- [20] S.G. Kim, Y. Otani, K. Fukamichi, S. Yuasa, M. Nyvlt, T. Katayama, J. Magn. Magn. Mat. **198-199**, 200 (1999).
- [21] T. R. McGuire and R. I. Potter, IEEE Trans. Magn. **MAG-11**, 1018 (1975).
- [22] Th. G. S. M. Rijks, R. Coehoorn, M. J. M. de Jong, W. J. M. de Jonge, Phys. Rev. B **51**, 283 (1995).
- [23] J.-E. Wegrowe, S. E. Gilbert, V. Scarani, D. Kelly, B. Doudin, J.-Ph. Ansermet, IEEE Trans. Magn. **34**, 903 (1998).
- [24] S. Wüchner, J. Voiron, D. Givord, D. Boursier, J. J. Préjean, J. Appl. Phys. **75**, 6682 (1994).
- [25] J.-E. Wegrowe, B. Barbara, V. S. Amaral, J. B. Sousa, J. Magn. Magn. Mat. **161**, 133 (1996).
- [26] I. Chlebny, B. Doudin, J.-Ph. Ansermet, Nanostructured Materials **2**, 637 (1993).
- [27] V. Scarani, B. Doudin, J.-Ph. Ansermet, to appear in J. Magn. Magn. Mat. (1999).
- [28] J.-E. Wegrowe, D. Kelly, A. Franck, S. E. Gilbert, J.-Ph. Ansermet, Phys. Rev. Lett. **82**(18), 3681 (1999).
- [29] R. Ferré, K. Ounadjela, J. M. George, L. Piraux and S. Dubois, Phys. Rev. B **56**, 14066 (1997).
- [30] S. Wüchner, doctoral thesis, Université Joseph Fourier, Grenoble France (1995).

- [31] A. Fert and D.K. Lottis in "Concise encyclopedia of magnetic and superconducting materials" Ian Evetts editor, Pergamon Press, p. 291
- [32] R. W. Cochrane, R. Harris, J. O. Strm-Olson, M. Zuckermann, Phys. Rev. Lett. **35**, 676 (1995).
- [33] D. L. Cox, A. Zawadowshi, Adv. Phys. **47**, 599-942 (1998).
- [34] H. Okuno, Y. Sakurai, J. Magn. Magn. Mat. **35**, 80 (1983), H. Okuno, Y. Sakurai, J. Appl. Phys. **53**, 8245 (1982), H. Okuno, Y. Sakurai, IEEE Trans. Magn. **17**, 2831 (1981).
- [35] B. Dieny, D. Givord, J. M. B. Ndjaka, J. Magn. Magn. Mat. **93**, 503 (1991).
- [36] P. Gaunt and C. K. Mylvaganam, Phil. Mag. B **44**(5), 569 (1981).
- [37] E. Köster in "magnetic recording technology" (C.D. Mee and E.D. Daniel. eds.) chapter 3, McGraw-Hill, New-York (1995).